C4-1472/3111
COPY
4

THEORETICAL ASPECTS OF METAL-ELECTROLYTE INTERFACES

FINAL REPORT

14 SEPTEMBER 1964

Prepared by:
V. W. Bolie
L. G. Bishop

Approved by:

V. W. Bolie
Chief, Bionics

J. W. Moyer
Director, Applied Research

Research, Engineering, and Reliability Division

Autonetics A DIVISION OF NORTH AMERICAN AVIATION, INC., ANAHEIM, CALIFORNIA

Subcontract 6625
Prime Contract NAS-4-566

CONTENTS

ILLUSTRATIONS

TABLES

I. SUMMARY OF RESEARCH RESULTS

Some typical electrode problems are outlined in Appendix I. An example is given to show the difficulties encountered in the use of conventional skin-surface electrodes.

Some experimentally observed bioelectrode characteristics are outlined in Appendix II. Skin surface electrodes, gross implantable electrodes and microelectrodes are discussed. Problems in their application are described, for both in-vivo and in-vitro applications.

Some considerations in designing electrodes for GSR measurements are present in Appendix III. Included is a discussion of some of the anatomical structures and physiological variables pertinent to the measurement of galvanic skin responses. Some practical design criteria for GSR electrodes are given, including electrode materials and paste compositions found to be useful by other investigators.

Some theoretical characteristics of chemical electrolysis cells are presented in Appendix IV, for the purpose of developing a better understanding of the behavior of metal-metal salt combinations such as Ag-AgCl. One important result is the prediction of a tendency of the electrolyte concentration (both anions and cations) to concentrate in the vicinity of one electrode, and to deplete in the region near the other electrode. It is possible that a large part of the skin-potential artifacts may be attributable to relative motions between the electrode and the skin surface at moments when the paste-electrolyte is non-uniformly distributed.

Some physical properties related to the measurement of electrical potentials are discussed in Appendix V. A salient point is that electrochemical potentials can be used to predict contact potentials at interfaces, and rate processes at the electrodes can be used to predict chemical electrode potentials. Attention is called to the point that if near-identical electrodes are used, and very low current is drawn through them, there will be a tendency for cancellation of artifacts. A new technique (using surface field-effect transistors) which shows promise for measuring skin potentials with much reduced artifact is outlined.

Some measurements on a copper-copper sulfate cell are presented in Appendix VI. It is shown that the system has reactive impedance and, surprisingly, exhibits a resonance at 210 cps. These results illustrate that a system previously considered rather elementary is

neither simple nor understood in terms of elementary theory. It is believed that the "negative resistance" characteristics may be due to differences between Cu^{++} and $SO_4^{=}$ mobilities.

II. SUGGESTED NEW AVENUES OF STUDY

This investigation has resulted in several new concepts which might be considered for additional study. Among these are the following:

1. From the basic point-of-view, additional studies are needed on the physical properties of interfaces, particularly solid-liquid junctions. It may be possible, through the deposition of special interface-coatings, to predict and control electrode potentials.

2. Additional in-vivo and in-vitro investigations, using various electrode materials, are needed to determine the electrode characteristics and their compatibility with living tissue. Consideration should be given to the problems that would be involved in developing a "transition material" which would provide a gradual alloy-taper from the copper-wire equipment-connections to the living tissues (perhaps easily oxidized metals at the wire, and weakly, non-toxic, redox chemicals at the skin surface). Further studies are needed to define more clearly the physical characteristics of the tissues to be contacted by the electrodes.

3. An extensive digital computer analysis of the nonlinear partial differential equations governing the transient interactions of skin surface electrodes with the electrolytes in the junction-paste and skin surface is needed. This study should span the frequency interval from 0 to 10 kc, and should include the effects of "partial polarization" induced by the flow of electrode current.

4. Special monitoring techniques should be developed to measure both slow and fast changes in interface characteristics of electrodes during their use in recording skin potentials. A more extensive search should be made to find suitable non-toxic ion types having equal mobilities to reduce the diffusion-potential voltages associated with recovery of uniformly distributed electrolyte compositions following bioelectric transients.

APPENDIX I

SOME TYPICAL SKIN-ELECTRODE PROBLEMS

Problems are encountered when there is a requirement for monitoring human bioelectric activity for periods longer than those normally encountered in clinical applications. These problems are increased when there is also a need for the subjects being monitored to function normally with minimum hindrance during this interval.

It may be pertinent to consider some of the problems encountered in bioelectric recording during a 5-man, 5-day simulated space flight conducted at WPAFB Aeromedical Laboratories in 1958. Conventional recording electrodes were used and periodic recordings of EEG, EKG, GSR, and respiration were carried out continuously for the 5 day period.

EEG electrodes were those normally used in clinical practice (Ag-Ag Cl and a saline paste). These were attached to the scalp with collodion-gauze. EKG was recorded through chromed plates and EKG electrode paste. They were held in place with a harness; respiration rate was obtained from the respiratory artifact present in this array. GSR was recorded through lead foot plates and EKG electrode paste. These were sewn into special stockings to obtain fixation.

Drying of the electrode paste required that the electrodes be removed, the area washed, and the electrodes repositioned with fresh saline paste at least every eight hours: frequently the interval was shorter. Electrode maintenance was performed by the subjects. Some skin maceration occurred secondary to long term contact with the electrode paste and the abrasive it contained. In spite of the care and labor invested in the maintenance of the electrode system the recordings were not satisfactory and were plagued with movement artifacts, transient induced potentials on the electrodes, and high impedance. No low frequency or DC-level information could be obtained, and the artifacts in the recordings were so numerous and obscuring that data reduction was almost impossible.

APPENDIX II

SOME EXPERIMENTALLY OBSERVED BIOELECTRODE CHARACTERISTICS

The application of body surface (skin) electrodes is usually preceded by what is euphemistically called "skin preparation." This may consist of brisk application of a solvent such as acetone; the "rubbing in" of an electrode paste; or, actual scarification of the superficial layers of the skin. All these methods effect the removal of the non-viable portion of the skin and permit electrode or electrode paste contact with viable cells of the skin. Scrubbing the skin with a solvent soaked surgical sponge abrades it. The electrode pastes contain an abrasive such as ground glass which makes minute scratches and direct scarification, of course, penetrates this non-viable layer. In actuality, these methods establish electrode contact with what may be considered the cells and tissue fluids of the body's interior. Electrode impedance and artifacts are often an indication of the degree to which this contact has, or has not, been established.

In view of the above, it is postulated that there is no schism between the basic characteristics of electrodes thus applied to the surface of the body, and those chronically implanted within it. The apparent difference is thought to have been engendered by the time the electrodes are in contact with the tissue. Implanted copper electrodes, in several weeks' time, produce marked tissue destruction while the same electrodes, applied to the body surface for an hour, produce no detectable damage. It is thought that long term monitoring of bioelectric activity with surface electrodes, will bring this particular problem into prominence; it is basic to electrode implants. Studies have shown that copper, silver, and silver chloride are not suitable for implantation.

Implanted electrodes may, however, be classified as to their physical efficacy in the manner in which they are used. In monitoring bioelectric activity with high-input-impedance amplifiers there is very little current through the electrodes. When electrodes are used for electrical stimulation, pulses of relatively high current density are passed through them. Thus, stainless steel, may be used to record bioelectric activity for months. However, when the same material is used as a stimulating electrode (as in an implanted cardiac pacemaker) the metal "plates out" into the tissue. This results in a fairly rapid physical destruction of the electrode. Platinum-10 percent Iridium on the other hand will conduct stimulating currents without such rapid destruction of the electrode.

Aside from tissue compatibility and the ability to retain physical integrity, there remains the fundamental problem of electrode function. An ideal electrode would be one which would conduct electrical signals to and from the tissue it contacts without distortion and without introducing artifact. Most, if not all, electrode materials and arrangements in current use fall far short of this ideal. The characteristics of the electrode and the electrode-tissue interface introduce varying components of charge, impedance, and probably rectification that alter the signals passed through it. The effect of these characteristics is to modify, obscure, and sometimes overhsadow the very measurements or stimuli that are desired.

While these effects occur at recording current levels it is simpler, as a first approximation, to consider some effects encountered at the higher current densities used in stimulation. Some work in this area has been conducted at the Oregon Regional Primate Research Center. Silver, gold, platinum-10 percent Iridium, and stainless steel, electrodes have been implanted in animals (monkeys and cats) and also have been studied in-vitro. Some general statements may be made of the results of these studies.

In the in vivo studies, a 100 cps sine-wave constant-current stimulator was used. This stimulator was especially designed to be capable of delivering constant pre-set current levels of 10^{-5} to 10^{-2} amperes (peak-to-peak) in trains of complete sine-waves beginning and ending at zero current (i.e., zero phase). Some of the observations were as follows. The dc resting potential of the tissue was found to be displaced during the stimulus, after which it slowly decayed to its former level over a period of minutes. The decay-time varied with the metal used, that of gold being shortest, platinum-10 percent Iridium the longest. The over-all-impedance of the electrode-tissue-electrode system changed during the first cycle of the stimulus and did not stabilize until several cycles later; there was usually some slight change throughout the stimulus. With repeated trains of stimuli at 2-5 minute intervals there was a persistent change of system impedance, usually to a lower value. This alteration was not present several days later, but could be reproduced (in quality) by repeating the stimulus pattern. The phase relationship between current and voltage continually shifted during the stimulus pulse train. This was more marked during the earlier part of a stimulus train. Stimuli of higher intensity produced more marked effects.

Lest the above effects be construed to be due to some property of living tissue, it should be noted that qualitatively the same observations were made with the electrodes immersed in physiological isotonic

saline (0.155N Na Cl). An attempt was made to study these effects in-vitro. The electrodes were immersed in saline and 10 cps to 10KC currents was passed through them. They were placed in a bridge circuit, and an attempt was made to balance the bridge with resistance and capacitance components. While a balance could be obtained at any given time, at a fixed frequency, the changing characteristics of the electrodes made it impossible to maintain a balance over a period of more than 5 minutes. The results were not numerically reproducible from day-to-day, nor could the trends of the electrode characteristics be predicted in advance.

Microelectrodes are used for recording the bioelectric activity of discrete small areas, either inside or outside cells. They may be divided into two types: metallic and liquid. The metallic electrodes are made of a fine metal core insulated, except at the tip, with a varnish or glass sheath. Point dimensions usually range from 1-10 microns and they are largely used for extracellular work. The metals commonly used are tungsten, solder, or a variant of Woods' metal. Electrode problems occur at the metal-tissue interface at the tip and are similar to those of gross metallic electrodes. Liquid filled electrodes consist of a glass micropipette filled with a conducting solution of ionized salts. The tip diameters range from less than 0.5 to 10 microns. The smaller diameters are satisfactory for intracellular applications. They present two problem areas: the fluid-tissue junction and the junction between the fluid and the stimulating or recording circuitry. Microelectrodes, because of the small conductor diameter inherent in their physical dimensions, introduce impedances of .5 to 100 megohms into the electrode-tissue-electrode complex. In addition, because of the thin insulating sheath, significant capacitance effects a are present in the electrode itself. The high resistive impedance of such electrodes requires amplifiers of very high input impedance.

From the above, it is apparent that there is a need for extensive investigations of the theoretical and experimental aspects of electrodes and electrode-tissue interface characteristics before quantitative measurements of bioelectrical phenomena may be accepted as reliable.

APPENDIX III

CONSIDERATIONS IN DESIGNING ELECTRODES FOR GSR MEASUREMENTS

In designing electrodes to measure a physiological entity such as galvanic skin response, it is important to have some understanding of the anatomical structures pertinent to the measurement. Also, design decisions may be influenced by the need to minimize the effects of other physiological variables which might otherwise obscure the desired measurement.

There are three physiological variables which may be detected at the surface of the skin by electrodes under suitable conditions. In 1890, Tarchanoff [1] reported that a sensitive galvanometer connected by non-polarizable electrodes to two skin areas in man registered a deflection when the subject was stimulated by touch, light, or auditory stimuli. He also observed responses when his subject was emotionally aroused or when mental effort was exerted. Tarchanoff's discovery was what is now known as the endosomatic skin response, an emf detected on the surface of the skin, especially in the palmar and plantar areas. Subsequent studies of the electrical properties of the skin lead to the discovery of two other skin parameters. The first, called basal skin conductance, G, is the real part of the admittance measured by applying an external source of electrical power to the skin. Basal skin conductance seems to be correlated with the general level of alertness of the subject [2], rising with increasing alertness and decreasing with drowsiness. When G is observed over a period of time, relatively small, transient-like changes are often noted in the conductance. These conductance transients constitute the other skin parameter called the galvanic skin response (GSR).

Figure 1 is a cross section of the human skin which illustrates the structures considered important in GSR studies.

The skin consists of a thin outer layer, the epidermis, and a thick inner layer, the corium. Under the microscope, three distinct regions of the epidermis may sometimes be distinguished. The outer horny layer is a porous network of coarse fibers which is easily penetrated by ions, large molecules, and even molecular aggregates. Medial to this is the stratum lucidium, a thin membrane which seems to be permeable to cations, but impermeable to anions. It is interesting to note that the stratum lucidium, according to Rothman [3]. . . "cannot be seen with sufficient clarity except in the skin of the palms

and soles...". These are precisely the regions where the exosomatic and galvanic skin responses are most pronounced. The third layer of the epidermis is called the Malphigian Layer. If substances from outside the body penetrate to the Malphigian Layer, the cells there present no obstacle to further penetration throughout the epidermis.

The corium is composed of loose connective tissue in which are found numerous capillaries, lymphatics, and nerve endings, and is passive to migration of ions through its substance. Also located in the corium are the roots of hair follicles, sebaceous glands, and sweat glands. Figure 1 shows that the gland ducts and hair follicles penetrate the otherwise continuous stratum lucidium.

Dye studies indicate that fluids applied to the surface of the skin penetrate the horny layer with ease, are blocked in the region of the stratum lucidium, but then penetrate into the Malphigian Layer and corium by paths through the walls of the hair follicles and gland ducts. The most important path in GSR studies is the path through the sweat glands.

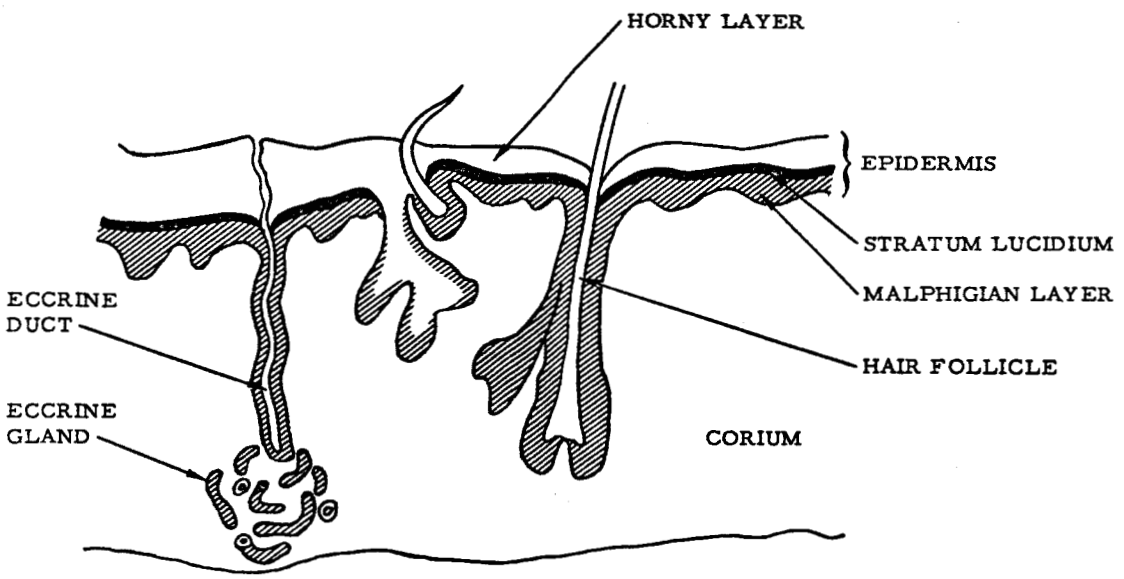

Figure 1. Cross Section of the Skin

In human skin there are two types of sweat glands, apocrine glands, and the more numerous eccrine glands. The apocrine glands are the older phylogenetically but have become rudimentary in man, whereas the eccrine glands have progressively become more important. In most mammals the eccrine glands are found only on the palmo-plantar surfaces. In lower primates, they have spread somewhat to other areas. In man, the eccrine glands are widely distributed, although they remain most dense in the palmar and plantar regions. The eccrine glands in these regions also differ structurally from those located elsewhere. According to Montagna [4], the glands of the palms and soles have a duct which is less than one-third the diameter of the secretory coil, making the transition between the duct and the gland somewhat abrupt, as in apocrine glands. Although not so prominent, the eccrine glands of the axillae also show this difference between the two segments. Elsewhere the differences in the diameters of the two segments are not so pronounced.

The eccrine glands of the human have two functions, the predominant function of a particular gland depending upon its anatomical location. In most regions of the body surface, the eccrine glands are thermoregulatory in function. However, the glands on the palmo-plantar surfaces appear to be less sensitive to temperature extremes. The sweating reactions of the palmo-plantar surfaces are thought to represent a facilitative reflex to assist in grasping responses and to increase tactile sensitivity in the face of a threatening situation. In some regions, notably the axillae, the eccrine glands seem to serve both functions with neither significantly predominant.

A. ENDOSOMATIC SKIN RESPONSE

As mentioned above, the endosomatic response is a transient emf which may be detected at the skin surface without using an external power source. In view of the impermeability of the stratum lucidium to anions, the existence of an emf between the skin surface and the deeper tissues comes as no surprise. The so-called injury potential which is observed between intact skin and a region where the skin has been broken is a salient manifestation of a steady-state emf.

The importance of being aware of the endosomatic response when designing electrodes for GSR measurements becomes obvious when the properties of the two phenomena are compared. The description of Tarchanoff's work revealed that the endosomatic response is elicited by the stimuli now known to elicit the GSR. Thus, if the autonomic nervous system controls the GSR as many now believe, it would be reasonable to assume that the endosomatic response is also

under autonomic control. According to Edelberg and Burch [5], the endosomatic potential has a time course similar to that of the GSR, and has an amplitude of up to eight millivolts. They further state that the polarity of the endosomatic response is such that it sometimes reduces the magnitude of the GSR and sometimes augments it. Wilcott [6] found a time lag between the endosomatic skin response and the GSR when he compared the two with the rate of palmar sweating. His experiment revealed that the latency of the endosomatic response following a stimulus is the same as that of the sweating response, whereas the GSR actually precedes the sweating response by about one second. This is not inconsistent with Edleberg and Burch's results, since the GSR duration is ordinarily several seconds. These considerations show that the endosomatic skin response constitutes a potentially troublesome sort of noise, since its frequency content is similar to that of the GSR and since it is elicited by the same stimuli. Fortunately, however, the endosomatic potential is independent of the current density at the measuring electrode, whereas the GSR varies directly with the current density. Thus, the artifact introduced by the endosomatic response is not appreciable if a sufficiently high current density is used for the measurements.

B. BASAL SKIN CONDUCTANCE

A preponderance of evidence indicates that the skin conductance is intimately connected with the ducts of the eccrine glands which provide shunt paths through the stratum lucidium. The sympathetic nervous system, in controlling emotional sweat secretion in the palmoplantar areas, seems also to control the conductance of these shunt pathways in an unknown manner. Since sweat ducts are apparently so important, let us view a single sweat duct as a unit of conductance, and examine the behavior of an ensemble of such ducts in parallel.

Edleberg and Burch [5], state that the apparent skin resistance is actually a polarization potential or back emf which is directly proportional to the current density in a certain region. Let us assume that a current of I amperes is delivered by a measuring electrode having an effective area of A cm^2. A potential, e, will then appear across the electrode terminals. The apparent skin conductance, G, is given by

$$G = \frac{I}{e} .$$

But, if e is related to the current density, J, by a constant of proportionality, k, we have

$$G = \frac{JA}{kJ} = \frac{A}{k}$$

Therefore, for all practical purposes, the sweat gland looks like an ordinary conductance between the external terminals.

In experimental work, conductances of the order of 2 μmho were observed between a pair of one-third cm^2 electrodes, giving an apparent conductance of 6 μmho per cm^2 of effective electrode area. Since there were sweat glands at each electrode surface in the experiments, a conductance of 12 μmho per cm^2 may be attributed to each skin surface. Therefore, a single sweat gland appears to have a conductance of the order of 0.03 μmho.

The value of the skin conductance, G, at any time is apparently an ensemble effect. Lykken [7] states that in ordinary sweating, the rate of sweat secretion of an area is a function of the relative number of glands active in that region at a particular time, rather than the secretion rate of individual glands. Thus a change in a central excitatory process causes a change in regional gland excitation, which in turn results in a change in the number of parallel conductance units. A useful result of this discussion is that an electrode of very large surface area will be adjacent to so many parallel conductance units that the effect at that terminal will be essentially zero. This makes it possible to study one skin-electrode surface at a time.

C. GALVANIC SKIN RESPONSE

Kling and Schlosberg [8] picture basal skin conductance as reflecting the subject's position on a continuum ranging from low to high activation, and the GSR as representing the subject's responses to stimuli of the moment. Sympathetic excitation of a region of the skin apparently switches a number of additional conductance units into the circuit for a short time interval, resulting in a GSR response.

Although there is still some variance of opinion in the literature about the sweat-gland explanation of the GSR, Rothman's summary of the evidence seems quite convincing.

"It was recognized early that sweat-gland activity is essential for this reaction. The supposition that smooth-muscle contraction plays a role in it has been abandoned, and participation of vasomotor impulses has never been satisfactorily evidenced. The reaction is abolished by peripheral nerve section or

by sympathetic ganglionectomy, an indication that the efferent part of the reflex is carried in sympathetic fibers. This alone, of course, would not exclude sympathetic vasoconstrictor impulses. However, Darrow, who simultaneously recorded galvanic skin response, plethysmographic changes, blood pressure, and accumulation of moisture on the skin surface, showed conclusively that changes in volume attributable to vasomotor responses were not related in any way to the occurrence or amplitude of the galvanic skin response. Moreover, the great majority of investigators found that atropization abolishes the reaction, a finding which at least strongly suggests the primary role of the sweat glands. It must be kept in mind that atropine has some vasomotor effects. The static resistance of the skin is influenced by atropine, and the psychogalvanic skin response is greater, the higher the static resistance. However, no reservation needs to be made in the evaluation of Wagner's observation. He found that the galvanic skin response could not be elicited in persons with congenital absence of eccrine sweat glands."

A troublesome problem arises in comparing various electrode designs used for GSR measurements, since the GSR waveform itself is not always constant in amplitude and duration. For proper evaluation of various electrode designs it is therefore necessary to control the excitatory state of the subject. A comparison technique conceived by Darrow [9] and used extensively by Edleberg and Burch [5] seems to eliminate this problem effectively. The technique consists of using two pairs of electrodes, each pair consisting of a small electrode and a very large electrode. The small electrodes are placed at two homologous sites, on corresponding forefingers for example. The large electrodes, which are in contact with essentially infinite conductance, are placed at any convenient site, such as the forearms, in order to form a return current path. By carefully adjusting the position of one of the small electrodes, a position may be found where the basal conductance levels and GSR responses of two identical electrodes are the same for long periods of time. After the electrode sites have been found in this manner, variables such as skin temperature, electrode area, electrolyte etc. may be studied at one of the electrode sites and compared with values obtained at the other site.

D. ELECTRODES

Since electrical conduction through the body utilizes ions, any external measuring system used in GSR studies requires interfaces between metals and ionic solutions. Lykken [7] stated that the appearance of an emf and a resistance is unavoidable at these interfaces, and

that the measurement problem amounts to choosing electrodes having small emf's, small variations in emf, and low internal resistances. He approached the problem by constructing electrolytic cells using a variety of electrolytes and a variety of electrode metals. His tabulated results are presented in Table 1. Lykken's conclusion was that the properties of zinc and lead make these materials most promising for use in GSR electrodes. Using these results, he designed several sets of GSR electrodes and obtained good, reproducible results.

In order to help prevent changes in the electrolyte concentration due to drying of the solution, and as a matter of convenience, it is advisable to use some type of electrode paste. Lykken's recipe for a zinc sulphate paste for use with zinc electrodes is given here.

> Mix together 30 gm. $ZnSO_4$, 60 gm. gum tragacanth, 85 gm. glycerin, and 600 cc. water. Heat in a double boiler for 2 hr, beat with an electric beater, heat again for 1 hr. Add 1 cc. carbolic acid and beat again until creamy.

One of Lykken's electrode designs utilized a scheme devised by Barnett [10] for eliminating contact impedance. Barnett's electrode, shown in Figure 2, utilizes an inner conductor to carry the current and an outer conductor for measuring potential with a negligible impedance drop.

Lykken stresses the importance of applying the electrodes to a clean, dry skin surface, in order to sharply define the effective surface area of the electrode and to obtain reproducible contact impedances. This view is shared by Edleberg and Burch who found that small quantities of sweat greatly interfered with measurements of both GSR and G.

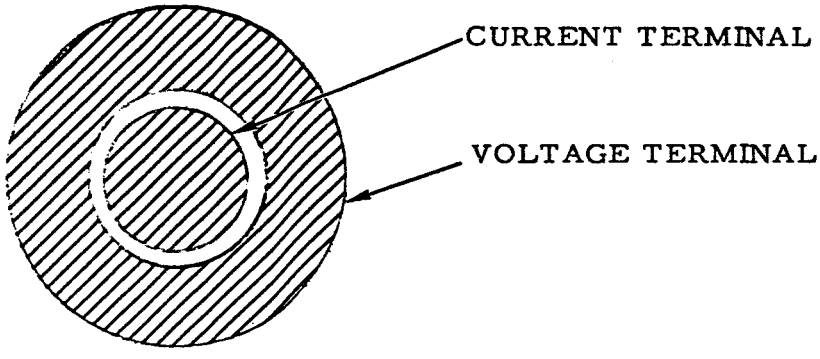

Figure 2. Two-Conductor GSR Electrode

Table 1

Spontaneous Potential and Apparent Direct-Current Resistance of Various Electrodes
(Measured from pairs of like electrodes in a saline cell)

Electrode		Spontaneous Potentials		Resistance at 50 Microamps	
Electrode Metal	Electrolyte	Mean During First Hour (mv.)	Variation After First 5 Min. (mv.)	After 10 Min. (ohms)	Variations in next 50 min. (ohms)
Stainless steel	NaCl	10	31	23,000	6,000
Zinc	NaCl	100	76	4,300	9,250
Zinc-mercury	NaCl	82	72	2,800	1,200
Zinc	$ZnSO_4$-NaCl	1	1	370	10
Zinc-mercury	$ZnSO_4$-NaCl	1	1	330	15
Silver	NaCl	94	28	23,500	1,000
Silver-mercury	NaCl	90	33	12,000	4,000
Silver	AgCl-NaCl	2.5	1	260	10
Lead	NaCl	1	1	800	18,700
Lead-Mercury	NaCl	1	1	19,000	3,000
Two-element lead	NaCl	1	1	30	1
Platinum	NaCl	320	205	37,600	22,400

Edleberg and Burch's experiments showed that although non-polarizable electrodes are necessary for accurately measuring basal conductance, polarizable electrodes give good results in GSR studies, where changes are to be measured. Edleberg tested electrodes of Ag, Fe, Cu, Pb, Al, Zn, stainless steel and solder connected to the skin by means of a 0.05 M Na Cl solution. He found that stainless steel and Al produce high random noise, solder, Ag, and Cu produce slow wave artifacts, but that Fe, Pb, and Zn are good materials for GSR studies. A recipe for a biologically inert Na Cl electrode paste having the salt concentration of average sweat was given by Edleberg and Burch and is repeated here.

> Six grams of corn starch (argo) are uniformly suspended in 100 cc. of 0.05 N. NaCl, and the mixture is brought to a boil while stirring. It is boiled gently for 30 seconds and poured into small vessels while hot (creamers are convenient) and capped; this last procedure prevents contamination by mold and subsequent hydrolysis. The preparation will remain stable for at least 10 days.

If Edleberg and Burch's conclusions concerning the acceptability of polarizable electrodes are correct, the NaCl electrolyte would offer a real advantage in not being diluted by sweat in long-term experiments. Of course, it would still be necessary to keep the skin dry in the region surrounding the electrode to insure a constant effective electrode area.

It was mentioned previously that a lower bound is imposed upon the current density used in GSR measurements by the necessity of obtaining GSR waves significantly greater in amplitude than the endosomatic skin response waves. There is also a practical upper limit to the current density which may be used. This upper limit is dictated by the possibility of injuring the skin by excessive values of current density. Edleberg and Burch [5] warn that current densities exceeding 10 $\mu a/cm^2$ produce an injury effect which is manifest as a non-linearity in the skin conductance. A compromise value for current density used by Edleberg and Burch was 8 $\mu a/cm^2$. A good discussion of skin injury is given by Mueller [11] et al, who also observed a very sharp nonlinearity in the electrical properties as current density was increased to high levels.

Figure 3 shows a GSR waveform obtained from the palmar surface using a pair of zinc electrodes and a 0.01 M $ZnSO_4$ solution. The effective electrode area was one-third cm^2 and the current density was 8 μamps per cm^2.

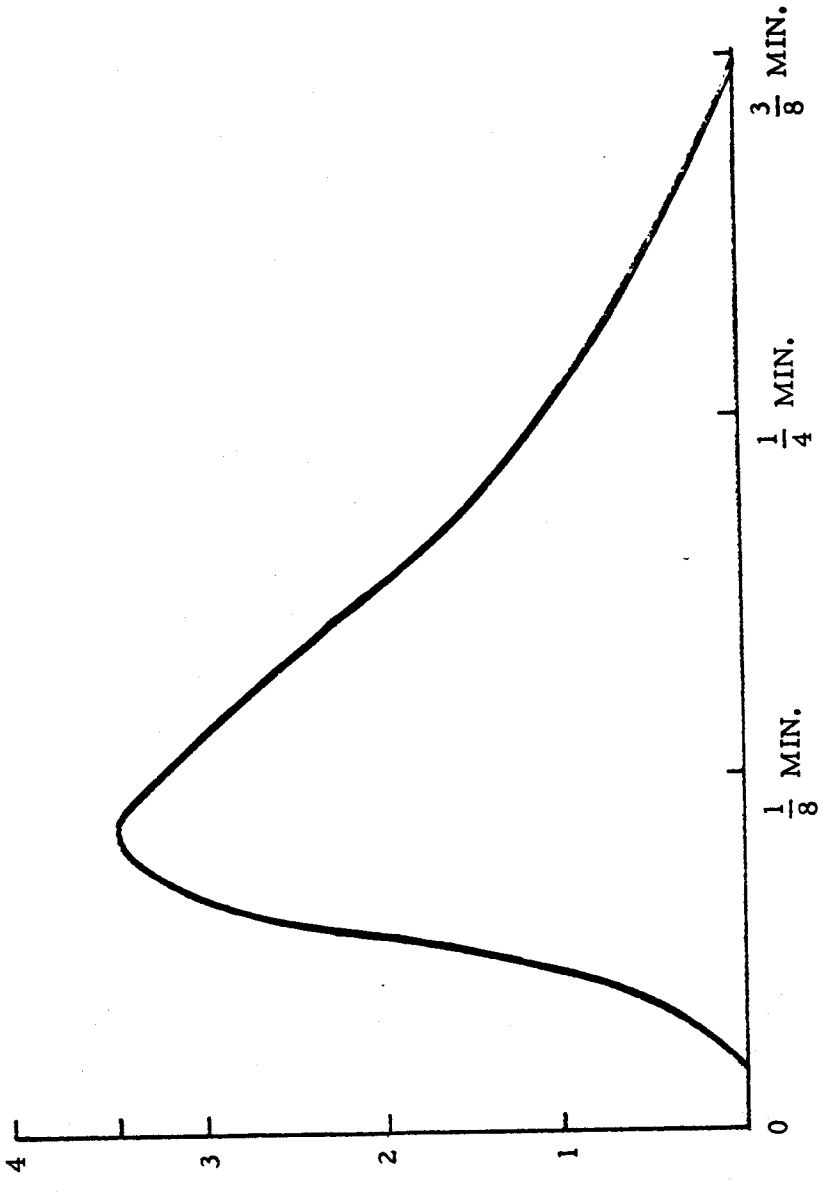

Figure 3. GSR Waveform

The fundamental frequency of the Fourier series for the GSR wave wave is of the order of 0.05 cps. The rise time of the wave is about 2.25 seconds, which means that a bandwidth of approximately 1.5 cps is necessary to faithfully measure the wave.

E. REFERENCES

1. Tarchanoff, J. Über die galvanischen Erscheinungen in der Haut des Menschen bei Reizungen der Sinnesorgane und bei verschiedenen Formen der psychischen Tätigkeit, Arch. f. d. ges. Physiol., 46: 46-55, 1890.

2. Hawkins, David R., Puryear, Herbert B., Wallace, Charles D., Deal, William B., and Thomas, Edwin S. Basal skin resistance during sleep and dreaming, Science, 136: 321-322, 1962.

3. Rothman, Stephen. Physiology and biochemistry of the skin, University of Chicago Press. Chicago. 741 pp. 1954.

4. Montagna, William. Structure and function of the skin, Academic Press. New York, 1962.

5. Edelberg, Robert and Burch, Neil R. Skin resistance and galvanic skin response, Archives of General Psychiatry, 7: 163-169, 1962.

6. Wilcott, R. C. Palmar skin sweating vs. palmar skin resistance and skin potential, Journal of Comparative and Physiological Psychology, 55: 327-331, 1962.

7. Lykken, David T. Continuous direct measurement of apparent skin conductance, American Journal of Psychology, 74: 293-297, 1959.

8. Kling, J. W., and Schlosberg, Harold. The uniqueness of patterns of skin conductance, American Journal of Psychology, 74: 74-79, 1961.

9. Darrow, C. W. The galvanic skin reflex (sweating) and blood pressure as preparatory and facilitative functions, Psychological Bulletin, 33: 73-94, 1936.

10. Barnett, A. The phase angle of normal human skin, Journal of Physiology, 93: 349-366, 1938.

11. Mueller, Emily E., Loeffel, Robert and Mead, Sedgwick, Skin impedance to pain threshold testing by electrical means, Journal of applied physiology, 5: 746-752, 1953.

12. Wagner, H. N. Jr. Electrical skin resistance studies in two persons with congenital absence of sweat glands, Arch. Dermat. and Syph., 65: 543-548, 1952.

APPENDIX IV

THEORETICAL CHARACTERISTICS OF CHEMICAL ELECTROLYSIS CELLS

A. INTRODUCTION

A rather extensive search of the literature in electrochemistry reveals that relatively little attention has been given to the electric field interactions between the reducible and irreducible ions in simple electrolysis cells carrying steady DC. In a $| Cu \| Cu^{++}, SO_4^{=} \| Cu |$ cell, for example, the electric field associated with the passage of DC will cause an "upstream" migration of the $SO_4^{=}$ anions to a non-uniform equilibrium distribution which involves a high concentration at the anode and a low concentration at the cathode. This non-uniform anion distribution couples in a complex manner with the otherwise-free cations in such a way that the electric field cannot be uniform, even in the case of "seeding" with inert salts such as KCl. Experimental Lissajous-figure volt-ampere patterns of such cells (1) prove that capacitance effects can be found even for "non-polarizable" electrodes.

The purpose of this paper is to present, as an initial theoretical attack on the problem, a mathematical analysis of the DC electric potentials and ion concentrations as functions of position in cells using parallel-plane electrodes. The simplifying assumptions are that all of the electrolyte is contained between the electrodes, that the space between the electrodes is free of stirring or convection, that the ions all have unit activities, and that the only ionic-driving forces are those of electric fields and diffusion gradients. The controlling equations have been justified and used to practical advantage elsewhere (2,3).

B. CELL WITH THREE BIVALENT ION TYPES

Useful insights to the general problem can be gained from a study of the three-ion cell, such as $| Zn \| Zn^{++}, SO_4^{=}, Mg^{++} \| Zn |$, in which only the bivalent electrode-metal cation is reducible, and the only inert-ion types present are a bivalent anion and a bivalent cation. A listing or primary nomenclature for this situation is given in Table 2.

When a steady electric current density J (amperes/meter^2) flows through the solution in the positive x-direction, it is carried by the reducible cations migrating from the anode on the left to the cathode on the right, while the inert ions assume concentration-distributions which equilibrate the diffusion and electric forces acting upon them.

Accordingly, the equations governing, respectively, the concentrations α, β, and γ of the reducible bivalent cation (e.g., Zn^{++}), the inert bivalent cation (e.g., Mg^{++}), and the inert bivalent anion (e.g., $SO_4^{=}$) are:

$$J = - p \left[2F\alpha \frac{d\phi}{dx} + RT \frac{d\alpha}{dx} \right] \tag{1}$$

$$\beta = \beta_A \exp(-2F\phi/RT) \tag{2}$$

$$\gamma = \gamma_A \exp(+2F\phi/RT) \tag{3}$$

$$\gamma - \beta - \alpha = \frac{\epsilon}{2F} \frac{d^2\phi}{dx^2} \tag{4}$$

The constants β_A and γ_A are the values of β and γ at the reference-potential point where $\phi = 0$. For algebraic convenience, this reference point may be located at the anode, which in turn can be located at x=0.

C. MATHEMATICAL ANALYSIS

Substitution of equations (2), (3), and (4) into equation (1) gives

$$\frac{d}{dx} \left(e^{2\theta} - \lambda^2 \left[\frac{d^2\theta}{dx^2} + \frac{1}{2} \left(\frac{d\theta}{dx} \right)^2 \right] \right) = - \frac{J}{2pRT\gamma_A} \tag{5}$$

in which

$$\theta = \frac{F\phi}{RT} \tag{6}$$

is the dimensionless electrical potential, and

$$\lambda_A = \sqrt{\frac{RT\epsilon}{4\gamma_A F^2}} \tag{7}$$

is a Debye-length. Since λ_A is a small length, of the order of a few tens of angstrom units, the solution of equation (5) is very nearly

$$e^{2\theta} = 1 - \frac{Jx}{2pRT\gamma_A} \tag{8}$$

which satisfies the boundary condition that $\theta = 0$ at $x = 0$. (It should be admitted here that equation (5) would contain both positive and negative exponential terms in the more complicated case where the ions are not all of the same numerical valency.)

If β_o and γ_o are the original concentrations of the inert cations and anions in the undisturbed cell, then

$$\frac{1}{b}\int_o^b \beta \, dx = \beta_o \tag{9}$$

and

$$\frac{1}{b}\int_o^b \gamma \, dx = \gamma_o \tag{10}$$

where b is the distance between the electrodes. Evaluation of these integrals, using equations (2), (3), (6), and (8) gives

$$\beta_A = \beta_o \frac{2J}{(J + J_m) \operatorname{Ln}\left(\frac{J_m + J}{J_m - J}\right)} \tag{11}$$

$$\gamma_A = \gamma_o \frac{J_m + J}{J_m} \tag{12}$$

in which

$$J_m = \frac{4pRT\gamma_o}{b} \tag{13}$$

is a collective quantity having the dimensions of a current density.

Substitution of equation (13) into equation (8) gives, for the formula describing the electrical potential as a function of position,

$$e^{2\theta} = 1 - \frac{2J}{J_m + J}\frac{x}{b} \tag{14}$$

Substitution of this result, together with equations (11) and (12), into equations (2) and (3) gives

$$\beta = \beta_o \frac{2J}{(J + J_m)\left[\mathrm{Ln}\,\frac{J_m + J}{J_m - J}\right]} \cdot \frac{1}{\left[1 - \frac{2J}{J_m + J}\,\frac{x}{b}\right]} \tag{15}$$

and

$$\gamma = \gamma_o \left[1 + \frac{J}{J_m}\left(1 - 2\,\frac{x}{b}\right)\right] \tag{16}$$

as the formulas defining the equilibrium distributions of the inert ions. Since terms as small as that on the right side of equation (4) have been neglected, it follows that the concentration of the reducible cations as a function of position is very nearly

$$\alpha = \gamma - \beta, \tag{17}$$

in which γ and β are described by formulas (14) and (15).

D. STATIC VOLT-AMPERE CHARACTERISTIC

The overall volt-ampere characteristic of the cell, as an electrical load connected to a DC potential source, can be obtained from equation (14) by applying the boundary condition,

$$\theta = -\frac{FV}{RT} \quad \text{for } x = b \tag{18}$$

and solving for J. The outcome of this procedure gives

$$J = J_m \tanh \frac{FV}{RT} \tag{19}$$

as the formula for the electrode current density resulting from the cell voltage V.

Equation (19) shows that the steady-state current density is a symmetric, but saturable, function of the applied DC voltage V, i.e., the current density is restricted to the range $-J_m \leq J \leq J_m$ for all possible voltages (below those of water electrolysis). For practical purposes, the current density can be considered as being at its

saturation level when V = 4 RT/F, i.e., when applied voltage is about equal to the "thermal voltage" multiplied by four. The physical reason for the saturation can be seen from equations (15), (16), and (17), which demonstrate that the concentrations of all three ion types in the vicinity of the cathode at x = b approach zero as J approaches J_m.

E. SUMMARY AND CONCLUSIONS

The foregoing analysis of the relationships between the cell geometry, ion concentrations, electrical potential, and current density, under conditions of steady electrodeposition covers the case in which the three ion types are all bivalent, with only one of the ion types being reducible. In the somewhat simpler case in which only two ion types are present, the cell formulas are:

$$J_m = 4pRTc/b$$

$$J = J_m \tanh (FV/RT)$$

$$\phi = \frac{RT}{2F} \operatorname{Ln} \left[1 - \left(\frac{2J}{J_m + J} \quad \frac{x}{b} \right) \right]$$

$$\alpha = \gamma = c \left[1 + \frac{J}{J_m} \left(1 - 2 \frac{x}{b} \right) \right]$$

in which c represents the electrolyte concentration existing in the cell before the steady current is applied.

As a numerical example, the simple cell, $| \, Cu \, \| \, Cu^{++}, \; SO_4 = \| \, Cu |$, may be considered for the case in which no cuprous ions are present. The typical values for the cell parameters as listed in Table 4 correspond to an effective Cu SO_4 average concentration of 0.043 moles/liter at 20 degrees centigrade and an electrode spacing of 0.5 centimeters. For these numerical values, the "thermal voltage" RT/F is 25.1 millivolts and the maximum current density J_m is 0.305 milliamperes per square centimeter.

The equations derived above provide some additional theoretical insight to experimental problems encountered in electrolysis. For example, Glasstone (4) makes the following comments:

> "It appears, from many observations concerned with electrolysis and other phenomena, that during electrolysis there is always immediately adjacent to the electrode a thin layer

> of solution in which there is a concentration gradient from that of the bulk of the electrolyte to the smaller or larger (for the cathode or anode, respectively) value at the electrode."
>
> "Concentration polarization can be diminished by increasing the rate of diffusion of the electrolyte, e.g., by vigorous agitation, by increasing the concentration of the solution, or by raising the temperature, but it cannot be entirely eliminated."

These observations are all predicted by the cell equations derived above.

A particularly important area of application of the foregoing theory is in the interpretation of bioelectric phenomena measured with skin electrodes or intracellular microelectrodes. The artifacts associated with such measurements are examined from an empirically-equivalent-circuit point of view in a recent publication by Weinman and Mahler (5); however, their study does not consider the influence of the electrolyte composition on the electrical transients. One strange transient effect predicted by the above equations may be found with the circuit shown in Figure 4. The switch may be assumed closed for a sufficiently long time to establish equilibrium (constant current) conditions in the cell and then suddenly opened at time t = 0. If the electrodes are copper and the electrolyte is $CuSO_4$, the microammeter would read zero immediately only if the Cu^{++} and $SO_4^{=}$ ions had exactly the same mobilities. In actual fact, the $SO_4^{=}$ ion moves 1.6 times as fast as the Cu^{++} ion in the same electric field. Consequently, the $SO_4^{=}$ ions will initially depart from the anode region at a faster rate than the Cu^{++} ions, with a resultant tendency for the anode to temporarily gain some positive charge -- even to the extent of producing a voltage "overshoot" under certain conditions. This principle may also help explain some of the "inductive" voltampere relations observed in electrical measurements of the squid axon, and helps explain the "negative resistance" frequently observed in Lissajous displays of the voltampere characteristics of electrolysis cells driven by low-frequency alternating currents.

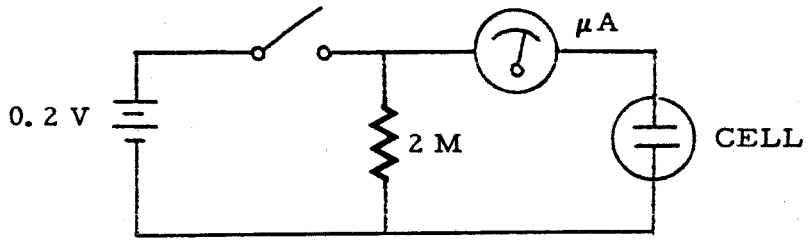

Figure 4. Circuit for Observing Transient Recovery of Zero Cell Voltage

Table 2. Primary Nomenclature

Symbol	Definition	Dimension
R	Gas constant (8.3)	joules mole $^{-1}$ degree $^{-1}$
T	Kelvin temperature	degrees
F	Faraday constant (96, 500)	coulombs equivalent $^{-1}$
ϵ	Water permittivity (0.71×10^{-9})	farads meter $^{-1}$
p	Mobility of reducible cation	meters ^{2} volt $^{-1}$ second $^{-1}$
α	Concentration of reducible cation	moles meter $^{-3}$
β	Concentration of irreducible cation	moles meter $^{-3}$
γ	Concentration of irreducible anion	moles meter $^{-3}$
x	Distance from left electrode (anode)	meters
b	Distance from anode to cathode	meters
J	Electric current density (uniform)	amperes meter $^{-2}$
ϕ	Electrical potential (zero at anode)	volts

Table 3. Secondary Nomenclature

Symbol	Definition	Dimension
α_o	Averaged value of $x\alpha$	moles meter $^{-3}$
β_o	Averaged value of β	moles meter $^{-3}$
γ_o	Averaged value of γ	moles meter $^{-3}$
λ_A	Debye-length for anode surface layer	meters
J_m	Maximum attainable current density	amperes meter $^{-2}$
c	Original concentration of reducible cation	moles meter $^{-3}$
V	Total voltage between electrodes	volts

Table 4. Typical Numerical Values for the Cell Parameters

Symbol	Numerical Value	Dimension
R	8.3	joules mole $^{-1}$ degree
T	293	degrees
F	96,500	coulombs mole $^{-1}$
p	3.6×10^{-8}	meters ^{2} volt $^{-1}$ second $^{-1}$
b	5×10^{-3}	meter
c	43	moles meter $^{-3}$

F. REFERENCES

1. Bolie, Victor W. and Langdon, Edsel M., "Chemical Electrode Voltampere Patterns," manuscript submitted for publication.

2. Bolie, Victor W., "The Biological Dielectric Paradox," Proceedings of the 16th Annual Conference on Engineering in Medicine and Biology, Baltimore, Maryland, November 1963, pp 158 - 159.

3. Bolie, Victor W., "Theoretical Finding of Transient Unbalance of Osmotic Pressure and Dielectric Tension," Nature, 201 (4915): 149 - 150, January 11, 1964.

4. Glasstone, Samuel, "Textbook of Physical Chemistry" Macmillan & Co., Ltd., London, Second Edition, 1960, pp 1013 - 1043.

5. Weinman, Joseph and Mahler, Jonah, "An Analysis of Electrical Properties of Metal Electrodes," Journal of Medical Electronics and Biological Engineering, 2: 299 - 310, 1964.

APPENDIX V

PHYSICAL PROPERTIES RELATED TO THE MEASUREMENT OF ELECTRICAL POTENTIALS

The problem of measuring the potential underneath a particular point at the surface of a body is an extremely complicated one. Many such measurements have been made, but little theory has been developed to aid in understanding the measurements. Thus, there is a question as to what is being measured and of what significance is the measurement? The purpose of this report is to discuss the first part of this question--what is being measured?

This report is divided into four sections, the first being concerned with concepts and definitions; the second with conduction in solids and liquids; the third with liquid-solid interfaces; and the fourth with the problem being considered of how to measure a skin potential and what is being measured. The sections are brief summaries with emphasis on the ties between physics, electrochemistry, and engineering applications emphasized.

A. CONCEPTS AND DEFINITIONS

1. Electric Potential

A most important concept is the concept of electric potential since this is what is being measured. Electric potential is associated with the work done, W, in moving a test charge, q_o, from one point to another, and

$$\phi = \lim_{q_o \to 0} \left(\frac{W}{q_o} \right) \tag{1}$$

where ϕ is the potential in volts if W is work in joules and q_o the charge in coulombs. In a static situation the potential of one point with respect to another is independent of the path through which the test charge moves. Thus, for a static situation, every point in space can be labeled with a potential with respect to some reference point, and often the zero potential point is chosen at infinity. It is experimentally difficult to measure potential by using a test charge. A finite quantity of charge must be used, and the presence of a finite charge affects the charge distribution in the volume of interest. Thus, potentials are usually experimentally determined by measuring current flows that result

because of the presence of a potential difference. However, the potential, as defined in Equation (1), must be carefully related to such currents. As an aid in understanding this comment, a brief discussion of the outer electric potential will be presented.

2. Outer Electric Potential

Consider an uncharged solid in a vacuum as sketched in Figure 1. In this situation the outer electric potential, zero in this case, is shown, and it is different from the internal potential. The difference is due to the presence of a dipole layer on the surface of the solid (assume it is a metal) caused by electrons with sufficient thermal energy to tend to leave the solid, leaving positive ions behind. The electrons do not leave because of the forces which hold them in the solid, image force and other forces such as valent bonding forces. The temperature dependent dipole layer (of the order of 10^{-4} cm.) causes an electric field as shown, and work must be done when the positive test charge is moved through this field to the interior of the solid. The magnitude of this potential difference is termed the Volta potential or tension (tension is defined so that it is equal to $-\phi$). Within the solid there are numerous mobile charges, electrons, so the potential within the solid is a constant for static conditions. If it weren't, the electrons would move in a manner to eliminate any potential differences. Figure 5 shows that positive charges can pick up energy due to the change in electric potential by moving from the inside to the outside of the solid. Because of this, one might expect the ions in the metal to move out, but this figure does not include interatomic forces which are much larger than the force associated with the Volta tension.

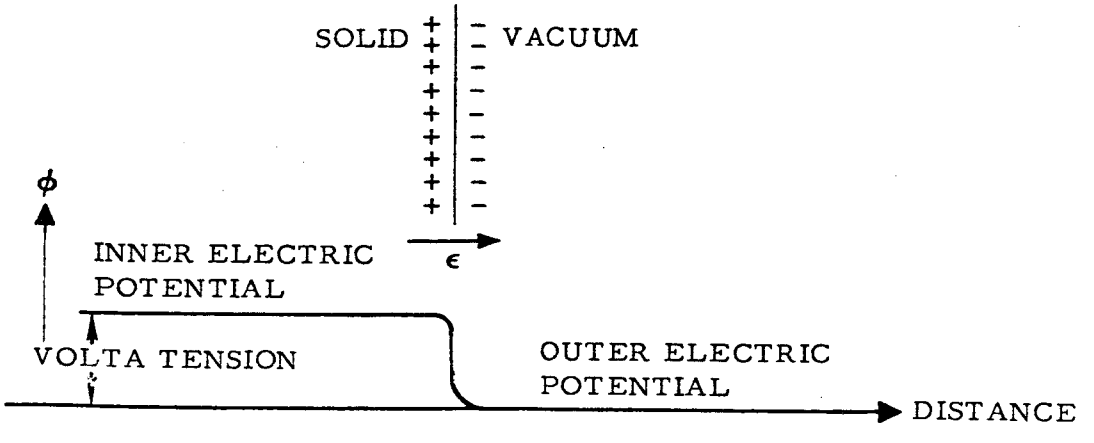

Figure 5. Potentials Near a Solid Vacuum Interface

3. Work Function

The carriers of interest within the solid are electrons, so to tie the concepts already discussed with concepts associated with conduction in metals, it is necessary to relate outside potential and Volta tension to work function. Figure 6 shows an electron energy diagram where E_v is the energy with respect to an arbitrary reference that an electron will have if it is at rest in the vacuum. The Fermi energy, E_F, is the energy some electrons will have within the solid. The probability of finding available quantum states at E_F filled is one half. The work function is the difference between the vacuum and Fermi energy levels. The Fermi energy is directly related to the electrochemical potential of electrons in the solid, and if E_v is chosen equal to zero, then the outer potential is zero, and

$$\overline{E}_F + W.F. = -E_F \tag{2}$$

where $\overline{E}_F$ is the chemical potential energy associated with work done when bringing an electron from infinity into the solid due to the chemical constitution of the solid. This work function definition holds in the absence of surface states.

Figure 7 reviews some of the concepts presented. Negative potential is plotted positive on the abscissa. The outer electric potential, ϕ_1, is determined by the free charge on the solid itself. The inner electric potential, ϕ_2, is determined by the surface dipole layer on the solid and ϕ_1. The chemical potential $\frac{\overline{E}_F}{q}$ is a function of

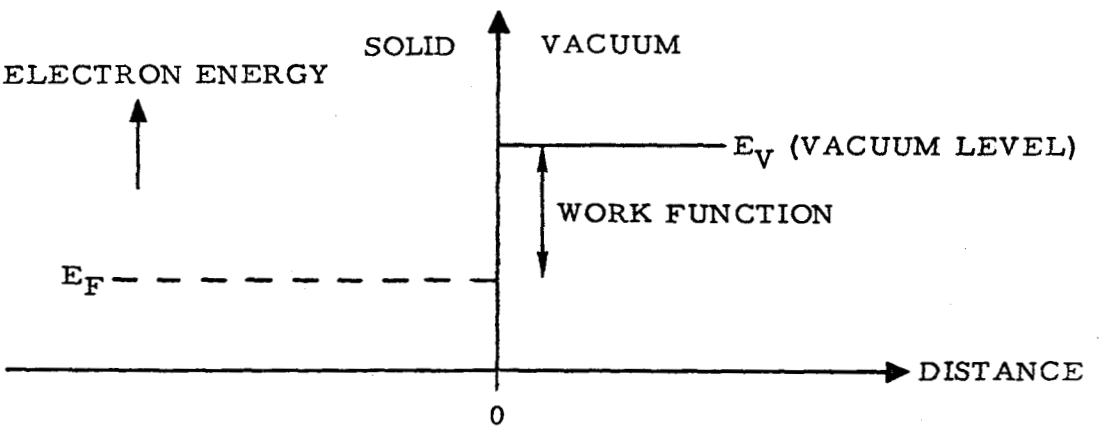

Figure 6. Electron Energy Diagram

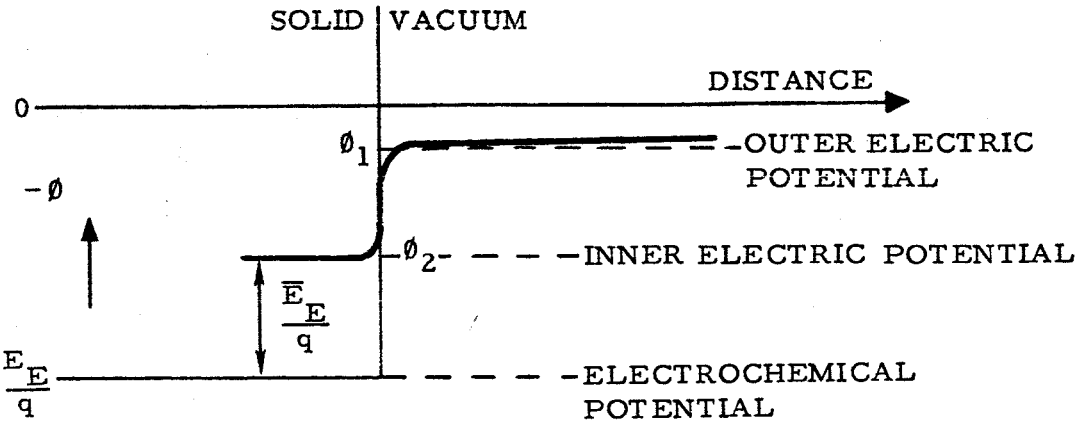

Figure 7. Potential Plot for Solid Vacuum Interface

the solid, and $\frac{E_F}{q}$ is the electrochemical potential. The energy necessary to raise an electron from the electrochemical potential to the zero or vacuum level is

$$W.F. = E_F = \overline{E}_F + q\phi_2 \tag{3}$$

and with no surface charges on the solid

$$W.F. = \overline{E}_F + q\phi_v; \tag{4}$$

Thus, the work function can be related to the Volta potential ϕ_v and the inner electric potential.

4. Contact Potential

Using the concepts just presented, it is informative to investigate the potentials expected if dissimilar metals are placed within a vacuum. Figure 8a shows two plots, one of electric potential and the other of energy as a function of distance within the evacuated chamber. In the

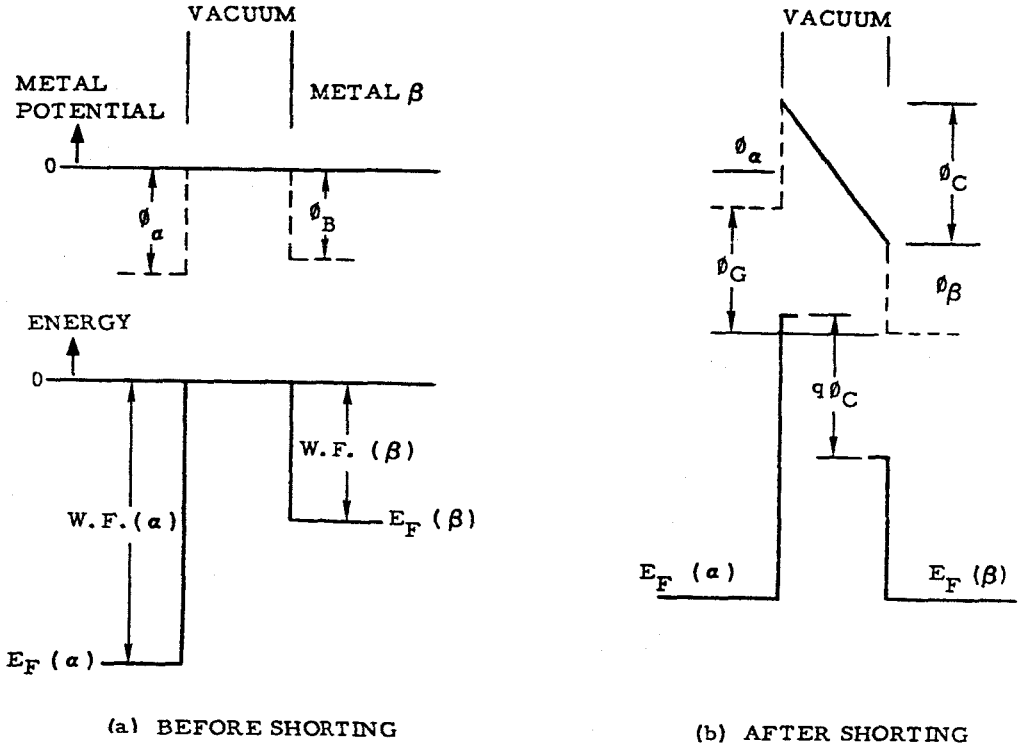

Figure 8. Contact Potential Concepts

top figure negative potential is plotted an ϕ_α is the inner electric potential of metal α with no free charge on it while ϕ_β is the inner electric potential of metal β and between the two metals there is no electric potential difference and thus no electric field in the vacuum. At the bottom of Figure 8a is a plot showing how the Fermi energies of these materials are related. Figure 7 shows the relations between the top and bottom parts of Figure 8a.

Assume a connection between metals α and β can be made external to the evacuated area by means of wires. Such a connection forces the electrochemical potentials $E_F(\alpha)$ and $E_F(\beta)$ to align themselves as shown in Figure 8b. The alignment is forced by the motion of electrons charging one metal at the expense of the other thus changing the outer electric potential of each. In this case electrons will flow through the

outside shunt from metal β to α for a very short period causing the outer electric potentials of metal α and β to differ by an amount

$$\phi_c = \frac{E_F(\alpha) - E_F(\beta)}{q} \tag{5}$$

where $E_F(\alpha)$ and $E_F(\beta)$ are the values of Figure 8a since in Figure 8b they are equal. The quantity ϕ_c is called the contact potential or the Volta tension, and there is an electric field in the vacuum

$$\epsilon = \frac{\phi_c}{d} \tag{6}$$

where d is the spacing between the metals. The field is from metal β to α and it is due to the surface charges on the faces of the metals. The Galvani potential, ϕ_G, is the difference between the inner potentials of the metals. In the case of metals with clean surfaces, the dipole layers are very small and the metals' inner and outer potentials are the same, so $\phi_c = \phi_G$ in that case. The various quantities discussed are useful for explaining what happens to potentials at interfaces, and what to expect when trying to measure potential differences. The concepts discussed have been applied to solids, however, the concepts of inner and outer electric potentials are applicable to liquids also, but the concept of work function is not in most cases since electrons are usually not the principal current carriers in liquids. In general, ions carry the current in liquids, and this is the case of interest here. However, a contact potential between a metal and a liquid is to be expected (non-vacuum situation) and this will be discussed in Section 4 of this report.

B. CONDUCTION

Conduction current at low frequencies is the rate at which charge moves through some area of interest. The charge motion may be voltage-generated, concentration gradient-generated, temperature-generated, light-generated, or generated by some other phenomena. At high frequencies, displacement current associated with a changing electric field may flow even though there is no charge motion in the region of interest.

1. Conduction in Solids

Conduction in metals generated by a potential difference is characterized by resistance

$$R = \frac{l}{A} = \frac{l}{\sigma A} \tag{7}$$

where the conductivity

$$\sigma = qn\,\mu_n;\ \frac{q = 1.6 \times 10^{-19}\ \text{coulombs}}{n - \text{carrier concentration}} \tag{8}$$

and the carrier mobility is such that

$$\hat{v} = \mu_n \epsilon \tag{9}$$

where $\hat{v}$ is the average electron velocity due to the applied electric field ϵ. The mobility can be computed since the electrons are accelerated for an average time, τ_a, by the electric field, and assuming they start with zero average velocity, then

$$F = m_e \frac{dv}{dt} = q\epsilon$$

$$S\emptyset\ \hat{v} = \frac{1}{2}\,\frac{q\epsilon\,\tau_a}{m_e} \tag{10}$$

where m_e is the effective mass of the electrons in the solid. The effective mass is different from the free mas due to the masking effect of the solid. The drift mean free path of the electron

$$h_d = \hat{v}\,\tau_a = \frac{q\epsilon\,\tau_a^2}{2m_e} \tag{11}$$

is the average length between collisions due to the applied field. At room temperatures the thermal velocities of the electrons are usually much much larger than the drift velocities and

$$h_t = \hat{v}_t\,\tau_a \tag{12}$$

is the mean free path between collisions with $\hat{v}_t$ the average thermal velocity of the electrons. In metals it is very difficult to initiate diffusion currents so they will not be treated here.

2. Conduction in Liquids

Electrolytes are the important liquid conductors and they can be solid or liquid. In the liquid form they are usually solutions, and the currents in these solutions are usually due to the motion of ions. The presentation here will be limited to liquid electrolytes with current flow due to ion motion implying mass transfer. The theory associated with such a situation is not well worked out nor experimentally verified. The reason seems to be that to generate conduction in electrolytes it is necessary to cause the current to flow through some type of interface, and even less is known of the interface characteristics.

However, the accepted explanation* is based on the theory of electrolytic dissociation which assumes that when an acid or base is dissolved in water, a considerable portion becomes spontaneously dissociated into positive and negative ions and these ions are free to move under the influence of an applied electric field. How they move will depend on the characteristics of the terminating interface because of the mass transfer aspects of the ion transfer. In other words, if the terminating interface is capable of accepting and furnishing ions of the proper type in large quantities, then the flow in the electrolyte is due to the motion of both types of ions. If only one terminating interface can furnish ions, then only that type of ion can furnish continuous flow. Thus, there are three limiting situations so far as d-c considerations are concerned: first when both ions are available, second when only one ion type is available, and finally when neither ion is available. Which case is present depends upon the terminating interface.

If the first situation is considered with ion concentrations $A^+ = A^-$ ions per m^3, then at every macroscopic point in the electrolyte there is electrical neutrality. Each ion is accelerated by an applied electric field. The velocity of the ion is by Stokes Law

$$v = \frac{zq\epsilon}{6\pi r\eta} \tag{13}$$

*Textbook of Physical Chemistry, Gladstone, Second Edition 1960, Macmillan Company

where η is the viscosity of the solvent, r the radius of the ion, zq the charge on the ion, and ϵ the electric field, so the ion mobility is

$$\mu = \frac{zq}{6\pi r\eta} \tag{14}$$

for this simple limiting case, and

$$\sigma_o = zq \left(A^+ \mu^+ + A^- \mu^- \right) \tag{15}$$

would be the predicted electrolyte conductivity if both ions can move freely and there is electrical neutrality. It should be noted that r may be different from that expected due to the ionic attraction of solvents. Also, this result assumes no interaction between ions and thus is the infinitely dilute condition. This then represents the expected conductivity for the conditions listed. Having a supply of ions available at the interfaces is not easily accomplished so this result is difficult to observe at d-c. However, at low a-c frequencies, the ions move back and forth thereby generating no mass transfer, so this result can be experimentally verified.

As the ionic concentration is increased from the infinitely dilute situation, the condition of electrical neutrality is violated in the vicinity of each ion since it will have more ions of an opposite charge in the vicinity, and this gives rise to the asymmetric and electrophoretic effects which depend on the ion concentrations. The result is

$$\sigma = \sigma_o - (A + B\,\sigma_o)\,\sqrt{C} \tag{16}$$

where C is the ionic concentrations and A and B are constants. Agreement with experiment is good for this result.

The other cases previously mentioned of only one ion's being available for conduction and none being available, give different results. In the last case, no d-c conduction takes place and the liquid acts like a dielectric. In the case of only one ion's being available, the concentration of the unavailable ion must vary with distance in such a manner that the diffusion force will offset the electric field. This results in a non-linear voltage-current relationship.

C. LIQUID METAL INTERFACES

The material presented is available from other sources, it has been reworded in a manner that will be useful in this discussion of liquid metal interfaces. There are two situations of interest: one in which no current flows through the interface, and one in which current flow is present. The first is the condition of interest when monitoring potentials with a high-impedance-measuring instrument, the second condition is of interest when stimulating by means of electrodes. Much of the material presented will be developed from the preceding theories, and it is therefore unavailable in similar form from other sources.

1. Static Conditions

In the case of no current flow through the interface, a useful analogy can be made to the discussion of contact potential given in Section A Par. 4. In that section the two separate clean metals α and β could have been brought in contact with each other rather than being shorted externally. If they were, there still would be an interchange of electrons, the establishment of a dipole layer at the interface, and the electrochemical potentials would be aligned. Thus, the outer electric potentials of the two metals would be different by the amount of the contact potential. This difference can be measured by an electrometer, but it cannot be measured by a voltmeter. A voltmeter measures differences in Fermi levels. Thus, this interface is not a source of useful potential difference even though a contact potential is present.

In the case of a metal-electrolyte interface, a contact potential is expected. However, this potential is not measured by usual techniques and, therefore, not a problem. The electrode potential due to the rates at which two opposing processes occur is a problem. One process is the passage of ions from the metal (or non-metal) into solution and the other is the discharge of ions in the solution forming metal (or non-metal) atoms on the electrode. In the case of a metal electrode, ions usually pass into solution more rapidly than they return resulting in the buildup of a potential barrier. If no current is allowed to flow externally, the electrode potential is sufficient to cause the two processes to have equal rates of occurrence. In this case there are four steps involved: the atom of the metal is vaporized, then ionized, dissolved in the solvent, and the electron returns to the metal. Thus, the electrode potential is determined by the heat of sublimation, the ionization potential, the work function, and the heat of solvation. Since only the heat of solvation is a function of the solvent, and it is relatively small, the ordering of the elements according to their electrode potential should be and is independent of the solvent.

In the case of a multi-interface arrangement, the total electrode potential is the algebraic sums of two potentials, one an oxidation potential and the other a reduction potential. Thus, knowing the materials and the electrolyte, it is possible to predict the electrode potentials.

2. Dynamic Conditions

In the case where the metal liquid interface carries d-c current, processes at the interface may limit the reaction. For example; the concentration of ions will change with respect to the static situation because of the net flow of ions past the interface. Thus, the electrode potential will not be a linear function of the current. In other words, the interface cannot be represented by a resistor-battery combination for all current levels. Only for small current densities can such a representation be used.

The current that flows through the interface will be due principally to the motion of ions. It is not expected that quantum effects, such as tunnel currents will play any part in the interface current flow.

D. MEASUREMENTS OF SKIN POTENTIALS

It is desirable to measure the electric potential between two points at the surface of the skin in a manner that is free of artifact.

1. Measuring Instrument

To measure potential differences it is apparent that wire leads to the points of interest must be included. These leads are connected to some measuring instrument. The instrument is sensitive to the difference between the electrochemical potentials or Fermi levels of the two leads. If the instrument is a very high-impedance device, then it can be energized by a contact potential. For example, if the two leads are made of different material, and if they are brought into contact with each other, there is a small transient motion of charge which a high-impedance instrument will sense as a reading. This reading will decay with time, but it will be troublesome. This is a disadvantage of a high-impedance-measuring instrument. An advantage of the high-impedance-measuring instrument is that little current will flow in the measuring circuit so that interface or electrode potentials are more easily predicted. Since the disadvantage is of a transient nature and the advantage long term, the indications are that a high-impedance-measuring device is desirable.

2. Contact Problems

The contact problems are many and varied. The first is that good electrical contact between the metal and the skin is desired. This implies the use of some electrolyte. The use of the electrolyte will introduce two more interfaces which will complicate the problem. Two possibilities are apparent: first to implant an electrode, or else to place the electrode directly on the skin surface.

If the electrode is implanted, it means discomfort, possible toxic action, and if a very tiny electrode is used, the potential will not be an average potential, but may represent the potential of a single cell only. The discomfort factor can be minimized by an extremely small electrode implanted in a relatively insensitive portion of the surface of the body. The toxic action can be avoided by choosing the metal carefully and by allowing no ion interchange by maintaining zero current flow. A small electrode might be useful, however, implanting is generally undesirable. It should be noted that the use of two similar electrodes of this type each generating a similar electrode potential should cause cancellation of the electrode potentials if the current is zero.

The second means of avoiding the use of an electrolyte is to apply a metal directly to the skin. This does not result in good electrical contact for any reasonable length of time. In such a case it is very important that the metal surface be clean and the skin must also be clean. However, the skin emits material, such as sweat, that causes problems so far as maintaining a clean surface is concerned. It would be easier to maintain a small skin area clean than a large one, however, to maintain good electrical contact in spite of motion and emission of contaminants, would be extremely difficult so this technique does not appear very useful.

Most present techniques involve the use of electrolyte interfaces between the metal and the skin. Most electrolytes are in the form of a paste. When using them it would again seem to be desirable to use a high-impedance-measuring device so little current will flow. Then the interface electrode potentials would tend to cancel out assuming similar metals are used at the electrolyte metal interface. The electrolyte skin interface is another complex problem which can be better understood using electrochemical approaches. Such an approach has not been found in the literature.

3. New Possibilities

It is apparent that considerable effort has already been expended to obtain artifact-free skin potential measurements. There are avenues of research which should lead to better measurements. The preceding sections dealt with techniques which will most likely result in good measurements. A question of interest here is what should be investigated for the future? This discussion will be limited to those techniques which will minimize the discomfort of the user which implies a small surface type probe.

It is known that the work function of materials, especially semiconductor materials, is a function of the condition of the surface of the material. It may be possible to design a material to have a good match to an electrolyte which in turn is well matched to the body.

A second, more interesting possibility, is to sense potential changes by some new technique. Figure 9a shows a device known as a surface field effect transistor. This consists of a piece of high resistivity P-type substrate with N-type material diffused into the substrate as shown. Ohmic contacts to the drain and source are shown as well as a thin silicon dioxide insulating layer. In usual applications, a metal is deposited on the oxide. In Figure 9b, the drain current I_D is plotted as a function of the drain to source voltage V_{DS} for various values of V_S. In usual applications V_S would be the gate voltage between the metal on the oxide and the drain. For the application envisioned, V_S would be the skin potential. With the device arranged as shown in C, the output would feed the measuring instrument.

The surface field effect unit operates on the principle that the potential applied to the outside of the thin oxide layer induces charges in the surface channel between the two N-type regions. The oxide layer is a good insulator so there will be no electrical interaction with the skin. The transistor has a large input impedance and can give amplification. Thus, the output can feed a relatively low-impedance-measuring device. The potential measured is between the point of contact of the field effect unit and the other probe, which could be a similar arrangement. The possibilities of this arrangement are intriguing.

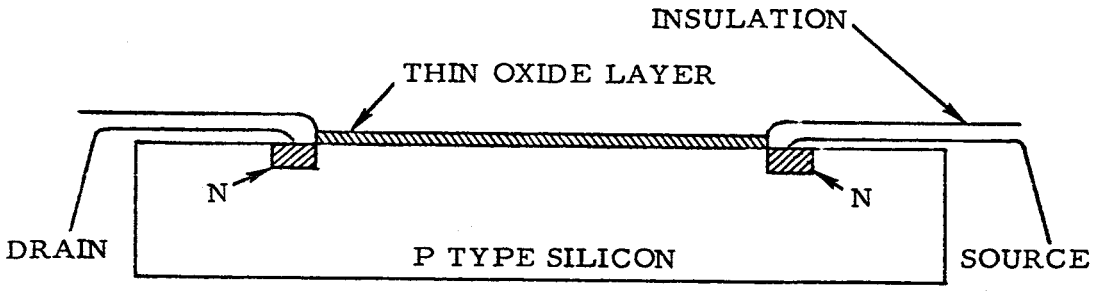

(a) DEVICE

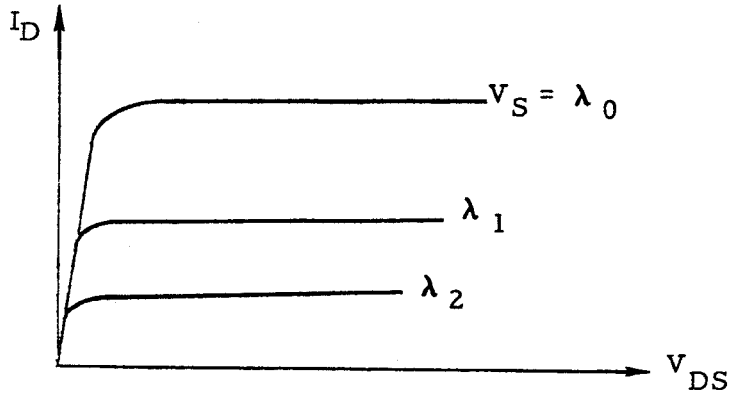

(b) CHARACTERISTIC

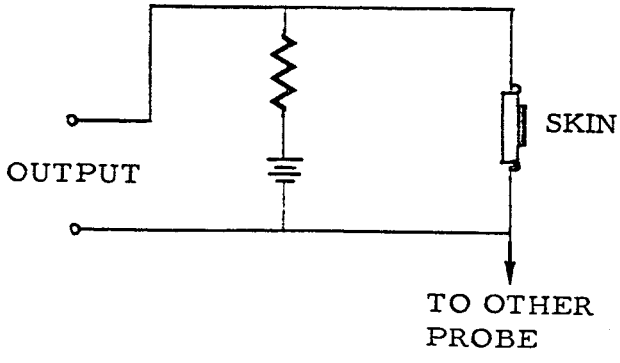

(c) APPLICATION

Figure 9. Surface Field-Effect Used to Measure Skin Potentials

APPENDIX VI

SOME MEASUREMENTS ON A COPPER-COPPER-SULFATE CELL

As yet an electrode system has not been devised that will record from (or stimulate) living tissue without perturbing the phenomena under investigation (Lily, 1961, Weinman and Mahler, 1964). Further, electrode characteristics are neither understood nor predictable. It is advisable, therefore, that experimental work accompany any theoretical considerations of electrode properties.

A limited investigation was made of a copper-copper sulfate cell. The results are presented in this section to illustrate the complexity that may be encountered in a presumably simple system.

The cell consists of two 5 cm.by 5 cm.plates made of copper foil bonded to fiberglass. These plates were placed 0.25 cm.apart in a lucite chamber containing one molar copper sulfate solution. Voltage-current characteristics were measured by applying constant-current square, triangular and sinusoidal input functions to the cell. All measurements were made with a Tektronix oscilloscope having 1 megohm input impedance. Plate polarity was changed frequently so that the plates would not become asymmetrical.

Hysteresis was observed over a wide range of frequencies (Figures 11, 12, 13). The system exhibited a resonance at approximately 210 cps (Figure 14). Several figures show a region of "negative resistance."

REFERENCES

1. Lilly, J. C., The Balanced Pulse-Pair Waveform, in Electrical Stimulation of the Brain, Ch. 6, Ed. Sheer, Texas U. Press, Austin, 1961

2. Weinman, J. and Mahler, J., An Analysis of Electrical Properties of Metal Electrodes, Med. Electron. Biol. Engrg., 2, 299-310, 1964.

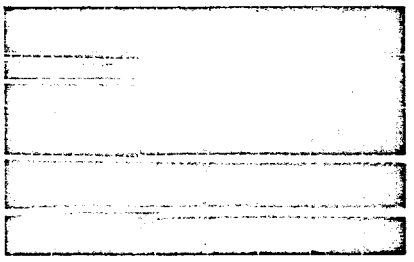

(a) I = 0.323 ma/cm^2, V = 95.0 mV

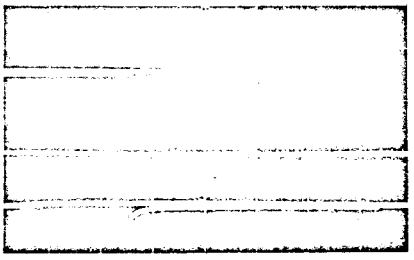

(b) I = .190 ma/cm^2, V = 77.5 mV

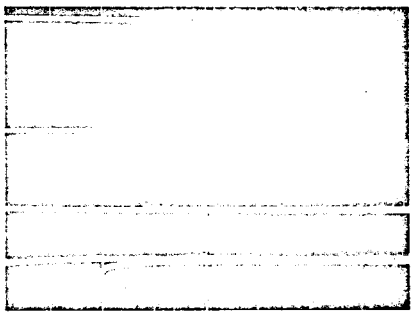

(c) I = .145 ma/cm^2, V = 72.0 mV

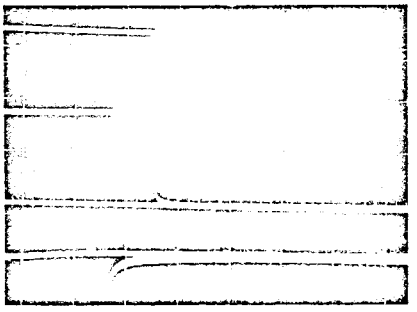

(d) I = .053 ma/cm^2, V = 66.0 mV

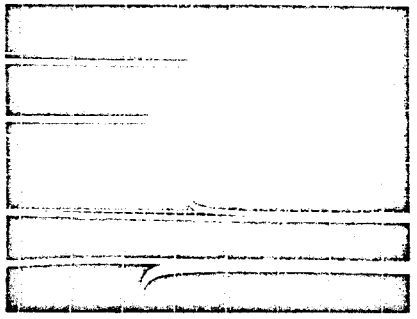

(e) I = .027 ma/cm^2, V = 57.0 mV

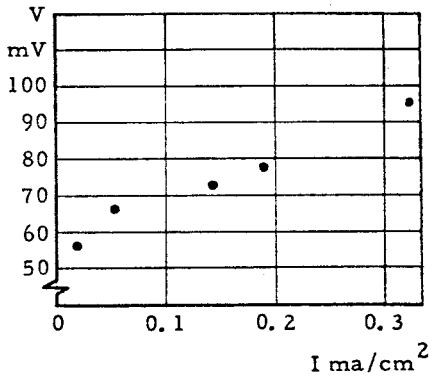

(f) CELL VOLTAGE vs APPLIED CURRENT

Figure 10. Voltage Measured Across Copper-Copper-Sulfate Cell as a Function of Applied Constant Current

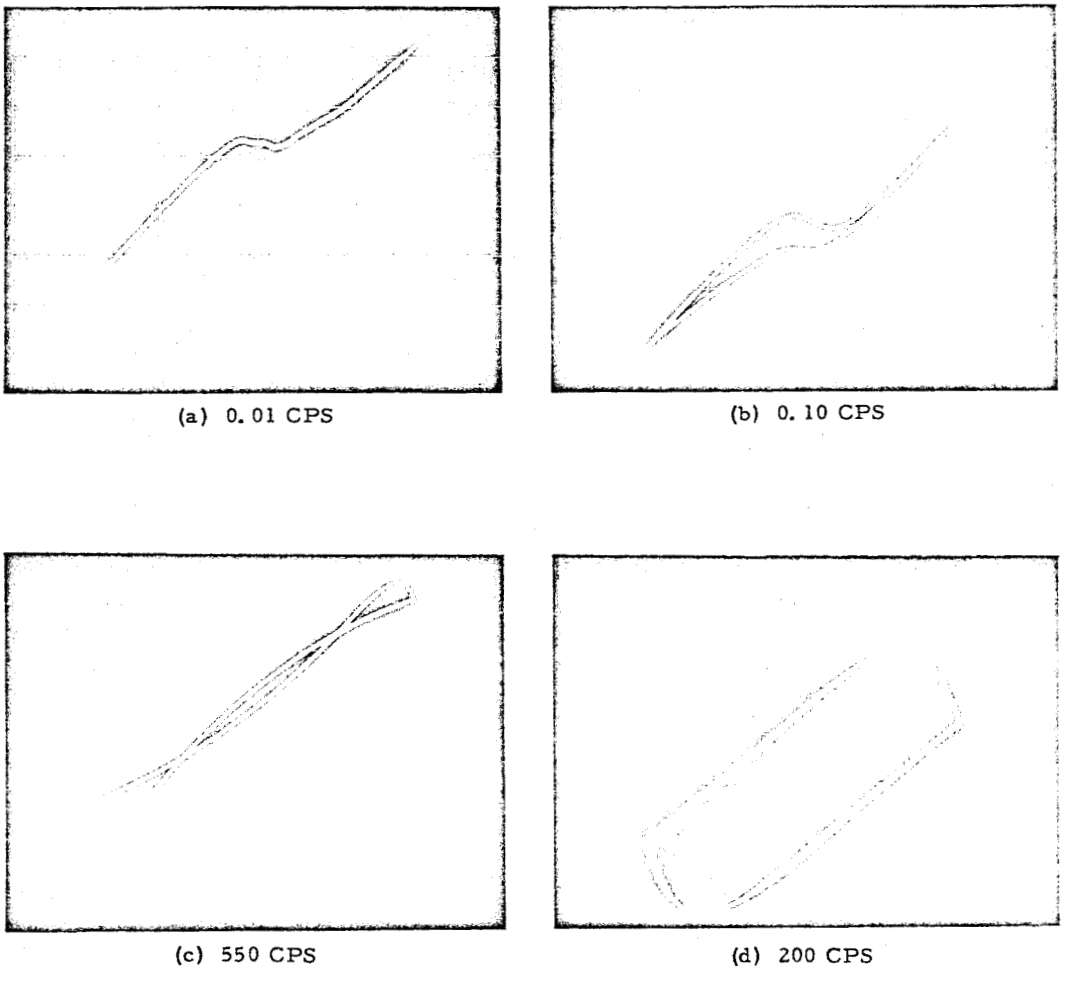

(a) 0.01 CPS

(b) 0.10 CPS

(c) 550 CPS

(d) 200 CPS

Figure 11. Measured Cell Voltage (ordinate) in Response to a Triangular Constant Current Driving Function (abscissa)

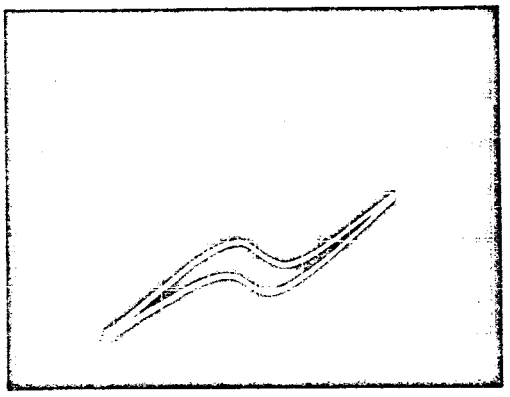

(a) 0.08 CPS

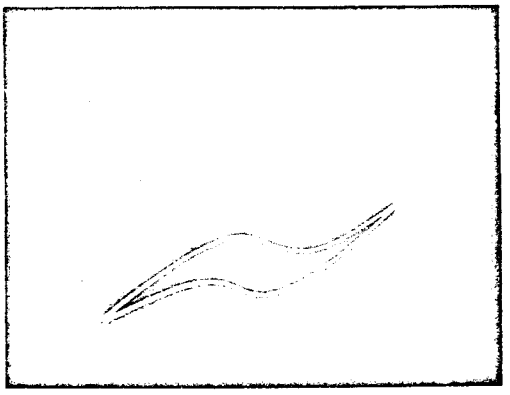

(b) 0.8 CPS

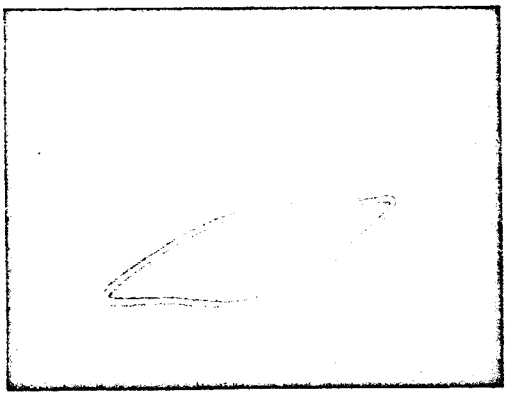

(c) 8 CPS

Figure 12. Cell Voltage (ordinate) vs Applied Constant Current Sinusoid (abscissa) Imax = 0.5 ma/cm^2

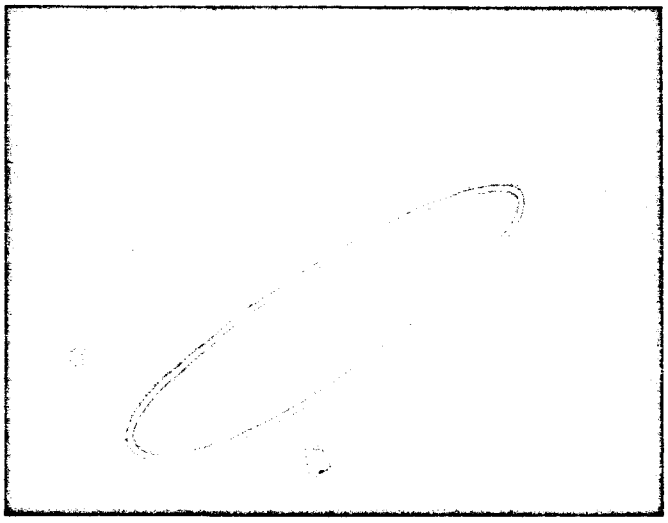

(a) 80 CPS

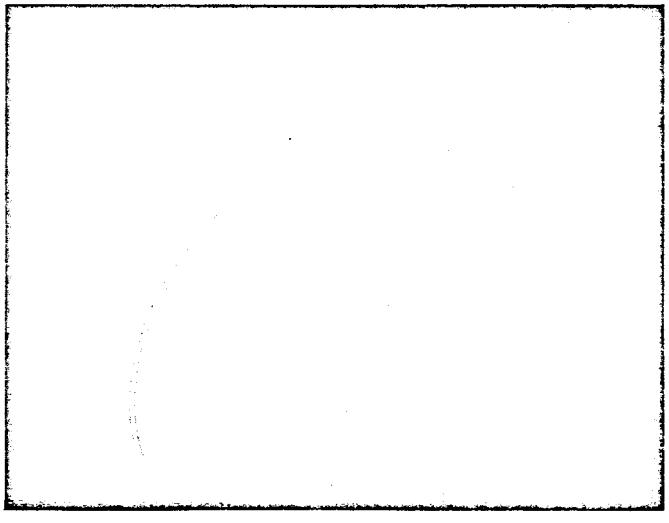

(b) 800 CPS

Figure 13. Cell Voltage (ordinate) in Response to Applied Constant Current Sinusoid (abscissa) Imax = 0.5 ma/cm^2

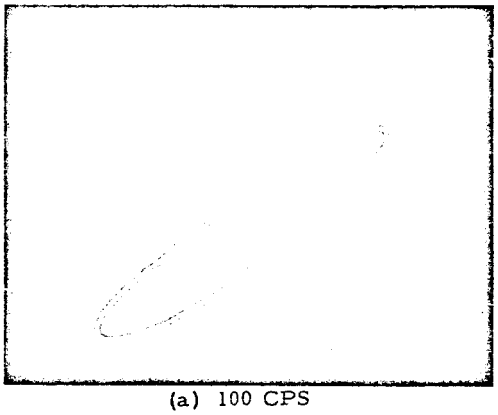

(a) 100 CPS

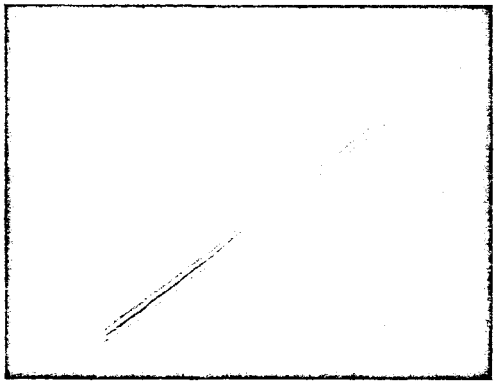

(b) 210 CPS

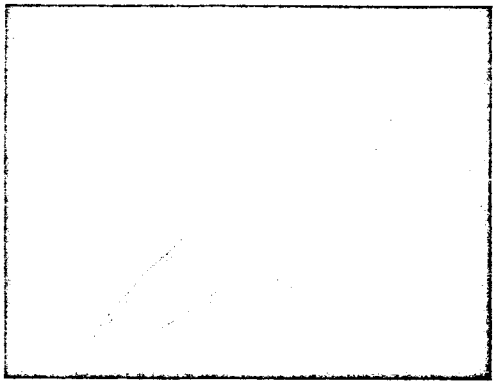

(c) 350 CPS

Figure 14. Cell Voltage (ordinate) in Response to Applied Constant Current Sinusoid (abscissa) Imax = 0.5 ma/cm^2